# Sinonasal Cancers

7

Roi Dagan and Curtis Bryant

## Contents



## 7.1 Introduction

Sinonasal cancers are among the most rare and diverse malignancies. They account for less than 3% of all tumors of the upper aerodigestive tract and less than 0.5% of cancers with an incidence in the United States of approximately 1 in 200,000 individuals annually [1]. There are many histologic subtypes including squamous cell carcinoma, minor salivary gland cancers (adenoid cystic carcinoma, adenocarcinoma, adenosquamous carcinoma, polymorphous low-grade adenocarcinoma, and mucoepidermoid carcinoma), neuroendocrine tumors (olfactory neuroblastoma, neuroendocrine carcinoma, sinonasal undifferentiated carcinoma, and small cell carcinoma), mucosal melanoma, lymphomas, and other cancers of mesenchymal cell origins such as chondrosarcomas and osteosarcomas. Essentially all evidence supporting management decisions come from retrospective studies, and with the

R. Dagan (✉) • C. Bryant
University of Florida Health Proton Therapy Institute, Jacksonville, FL, USA
e-mail: rdagan@floridaproton.org



N. Lee et al. (eds.), *Target Volume Delineation and Treatment Planning for Particle Therapy*, Practical Guides in Radiation Oncology,
https://doi.org/10.1007/978-3-319-42478-1_7

exception of lymphomas, surgery and radiotherapy is the mainstay of local therapy, which is guided by the following principles:

1. Cancers of sinonasal region are typically diagnosed at a locally advanced stage and are highly infiltrative with a high propensity for involvement of adjacent sinonasal cavities, orbit(s), skull base bones/foramina, or the intracranial compartment. At least 50% of patients will have tumors involving more than one anatomic subsite, and orbital invasion has been reported in 10–37% [2, 3]; cranial nerves are involved in as many as a third of patients [4], and intracranial invasion in up to 45% [3]. The locally invasive nature of these cancers underscores the importance of adequate wide-field local therapy to achieve optimal outcomes.
2. Combined modality therapy including gross total resection, via either an endoscopic or open approach, with postoperative radiotherapy has resulted in the best outcomes. However, the ability to use radical surgery and radiotherapy to eradicate local disease is limited by the tolerance of adjacent critical normal tissues (eyes, visual pathways, cranial nerves, brain stem, and brain). Serious visual pathway toxicities have been reported in over one-third of patients treated with conventional radiotherapy [5]. Many patients with intracranial disease extension will be at risk for developing radiographic and possibly symptomatic CNS effects from radiotherapy. Nevertheless, treatment intensification with dose escalation, and/or radiosensitizing chemotherapy, can potentially improve outcomes and has grown in use.
3. Local disease control is the major determinant of morbidity and mortality. Local-control rates historically ranged from 50 to 60% at 5 years with conventional radiotherapy and minimally improved to 68–75% with intensity modulated radiotherapy (IMRT). These rates closely approximate disease free and overall survival rates. Distant metastatic spread of tumors is rare with continuous local-regional control of disease occurring in 15–20% of patients, and thus, continuous local tumor control has been shown to be associated with a fourfold decrease in the risk of death [3].

Because of the challenges of delivering aggressive doses with conventional radiotherapy, proton therapy has been used extensively at centers worldwide for sinonasal cancers. The physical advantages of particle therapy can serve as a means of facilitating treatment intensification [6]. Recently reported outcomes, including a systematic review and meta-analysis, have demonstrated that proton therapy improves disease control compared with conventional RT and IMRT. The following chapter will guide readers through the treatment planning considerations for proton therapy.

## 7.2 Immobilization/Simulation

Patients are immobilized supine, typically on a board such as a base of skull frame, with a moldable cushion supporting the neck and helping reproduce neck extension, and a thermoplastic mask. This allows the neck and head to be extended off of the

treatment table, which minimizes the potential for collisions even when treating with oblique angles, and it minimizes the air gap between the snout and the patients which reduces the lateral beam penumbra. Oral obturators/stents can be used to depress the tongue and displace a significant amount of oral cavity mucosa from the treatment field. Treatment planning CT images should include the vertex through the shoulders, which can sometimes be a source of potential collisions, and the primary treatment planning images should be free from any material that could affect the dose modeling by altering the stopping power of the native tissues. For example, IV contrast, while helpful in target and organ at risk (OAR) delineation, should not be included in the primary image set. If possible, patients should have their sinonasal region cleared of all postoperative secretions and debris, and this should be maintained throughout the treatment course.

## 7.3 Target Volumes

Treatment planning should be based on pre- and postoperative imaging (CT and MRI) and operative/endoscopic findings. MRI should include high-resolution, contrast-enhanced T1-weighted imaging including fat suppression, and T2-weighted imaging is also very helpful in differentiating benign mucosal secretions and mucoperiosteal thickening from tumor involvement. Dedicated coronal images can also be very helpful. CT imaging for both diagnostic and treatment planning studies should be acquired with and without IV contrast and dedicated high-resolution bone imaging can aid in accurate target definition.

In both the primary and postoperative setting, the primary site is considered at high risk for recurrence regardless of the extent of resection. We recommend targeting two separate clinical target volumes (CTVs) based on the risk of residual disease. These targets can be treated with either a sequential boost approach or an integrated boost approach. The latter approach is facilitated by the use of pencil-beam scanning intensity modulated proton therapy (IMPT). However, if a hyperfractionated dose-fractionation schedule is preferred, then a two-phase sequential boost is recommended. Either way, the following approach is used to define the target volumes:

1. The gross tumor volume (GTV) is contoured on simulation CT/MR images and co-registered diagnostic scans, and in the setting of prior resection, a pre-opGTV is contoured on co-registered preoperative CT and/or MRI. Incorporating all available information from endoscopic evaluations, diagnostic CT and MR imaging, and operative findings is critical for accurate delineation of the GTV or pre-opGTV. Examples of pre-opGTV are shown in Figs. 7.1 and 7.2.

The initial target, standard-risk clinical target volume (CTV SR), includes an expansion of the GTV or pre-opGTV. For the most common scenario of a nasal/ethmoid primary tumor, we recommend including the entire nasal cavity, the contiguous involved paranasal sinus tissues, adjacent skull base, and the adjacent

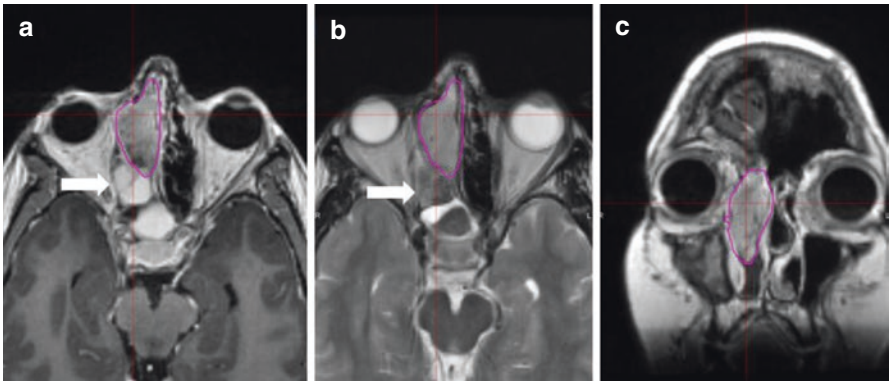


**Fig. 7.1** Diagnostic preoperative MRI of a T3 N0 M0 right naso-ethmoidal sinonasal intestinal-type adenocarcinoma. (**a**) Contrast-enhanced axial T1-weighted image. (**b**) Axial T2-weighted image. (**c**) Contrast-enhanced coronal T1-weighted image. Note that both T1- and T2-weighted images are useful in distinguishing tumor from benign mucosal secretions (*arrows*), which is often characterized by high-intensity T2 signal. However, in this case, these secretions contain proteinaceous material and also appear low intensity on T2. The pre-opGTV is outlined in the *magenta contour*

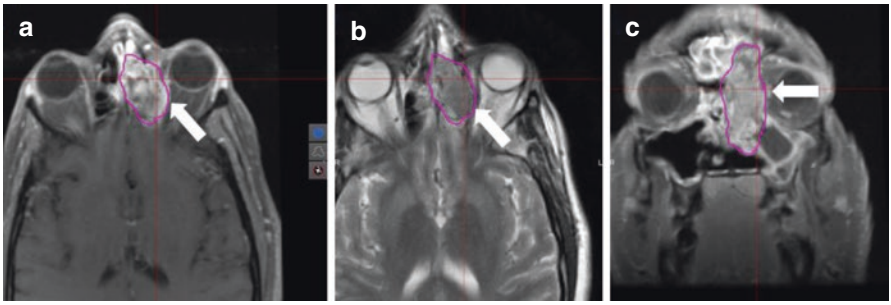


**Fig. 7.2** Diagnostic preoperative MRI of a left naso-ethmoidal T4a N0 M0 high-grade adenocarcinoma with invasion of the frontal sinus and left orbit. (**a**) Contrast-enhanced axial T1-weighted fat-suppressed image. (**b**) Axial T2-weighted image. (**c**) Contrast-enhanced coronal T1-weighted fat-suppressed image. Note the minimal intraorbital invasion (*arrows*) resulting in mild left proptosis. Invasion of the periorbita is best demonstrated on fat-suppressed images. The pre-opGTV is outlined in the *magenta contour*

periorbita and dura in cases where there is intraorbital or intracranial extension, respectively (Fig. 7.3). The CTV SR expansion varies based on the extent and location of the GTV or pre-opGTV, but for a lateralized naso-ethmoidal tumor or maxillary sinus primary tumors, this volume usually does not extend to the contralateral maxillary sinus or superior 1/2 of the frontal sinuses in tumors that do not cross midline or grossly extend into the frontal sinuses. This expansion will also vary widely with respect to the GTV/pre-opGTV on any given axial slice ranging from as low as 0 mm when the target volume approaches but does not invade the intracranial or intraorbital compartments to as wide as an entire maxillary sinus (2–4 cm)

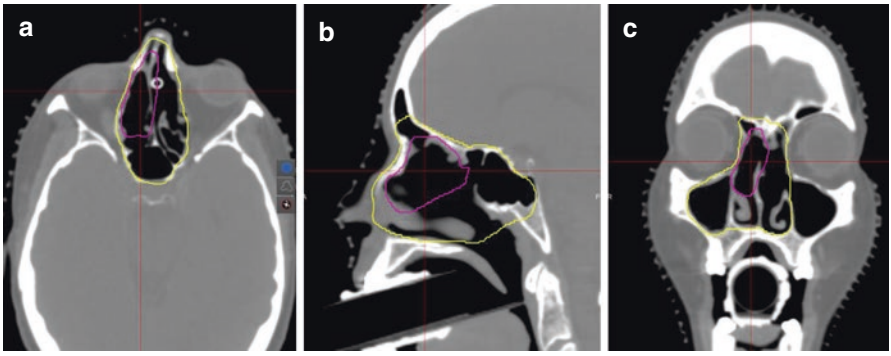


**Fig. 7.3** Planning CT of a T3 N0 M0 right naso-ethmoidal sinonasal intestinal-type adenocarcinoma. The pre-opGTV is outlined in the *magenta contour*. The CTV SR (*yellow contour*) includes the entire nasal cavity, the contiguous involved paranasal sinus tissues, and adjacent skull base. Since there was no orbital or intracranial invasion, there is a minimal CTV margin along these boundaries. Since the right middle meatus was involved, there is a generous margin including the entire right maxillary sinus

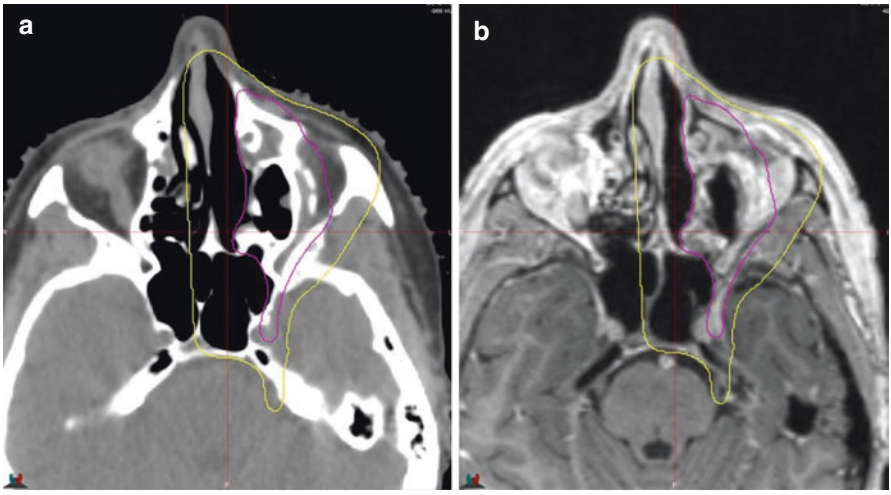


**Fig. 7.4** Planning CT and MRI of a left maxillary sinus squamous cell carcinoma with clinical and radiographic perineural invasion of right V2 to the cavernous sinus. The GTV is outlined in the *magenta contour*. The CTV SR is outlined in the *yellow contour* and includes the entire cavernous sinus, trigeminal nerve root as it enters the brain stem, and the retroantral space

when covering an adjacent but uninvolved maxillary sinus with a primary naso-ethmoidal cancer.

In cases, where there is clinical or pathologic perineural spread, we recommend treatment of potentially affected skull base foramina, the cavernous sinus, and nerve roots to the brain stem (Fig. 7.4). In cases where nodal irradiation is indicated (discussed later), then the upper neck nodal regions (uppermost retropharyngeal and retrostyloid nodes) are incorporated in the CTV SR. Lastly, in the postoperative

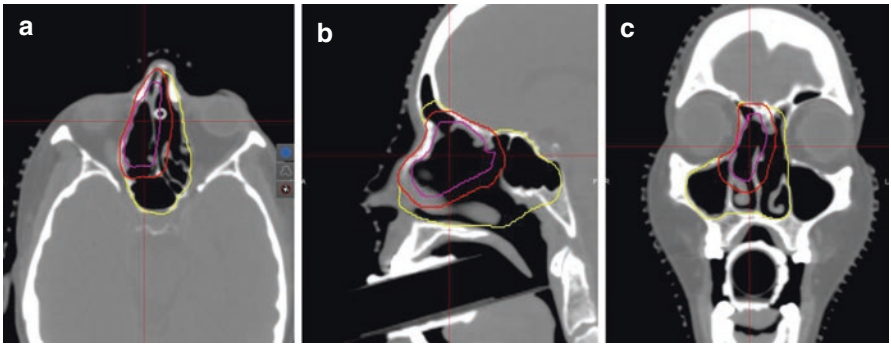


**Fig. 7.5** Planning CT of a T3 N0 M0 right naso-ethmoidal sinonasal intestinal-type adenocarcinoma. The pre-opGTV is outlined in the *magenta contour*. The CTV HR (*red contour*) is a 5–10 mm expansion of the pre-opGTV confined to the CTV SR (*yellow contour*)

setting, when an open surgical approach is used, then the surgical scars should be incorporated in the CTV SR. This includes the bicoronal craniotomy incision in patients who undergo craniofacial resection.

2. The boost volume or high-risk clinical target volume (CTV HR) is defined as a customized 0–10 mm expansion of the GTV/pre-opGTV and is limited to the CTV SR. This expansion will depend on the risk of subclinical disease in the region, whether the expansion region is extended along tissue at risk for invasion or into a non-invaded compartment (Fig. 7.5).
3. PTV margins will vary among institutions based on equipment specification and immobilization and image-guidance modalities. Typically margins of 3 mm are applied to create the final target volumes.
4. Additional proximal and distal margins are applied based on beam-specific parameters.

## 7.4 Dose/Fractionation

Currently, there is no standard dose/fractionation regimen for sinus and nasal cavity cancers. Generally, the PTV HR is prescribed 66–70 Gy (RBE) at 2 CGE per fraction, and 45–50 Gy (RBE) are prescribed to the PTV SR. In many cases, one or both visual pathways are intimately associated with the PTV HR, placing patients at significant risk for vision loss from retinopathy or optic neuropathy. In these cases, we prefer to use hyperfractionated therapy. In this scenario we prescribe 45.6–50.4 Gy (RBE) to the PTV SR and 69.6–74.4 Gy (RBE) to the PTV HR. Hyperfractionation accomplishes two goals that may improve outcomes. First, hyperfractionation can be used to accelerate RT to combat accelerated repopulation of tumor cells after surgery and during RT [7]. Second, using a lower dose per fraction allows for dose intensification while reducing the risk of visual pathway toxicity [8, 9]. Plans are typically normalized to ensure coverage of 95% PTV SR with

100% of the prescribed dose ensuring that 99% of the PTV receives 93% of the prescription dose to minimize any potential cold spots. The boost phase is normalized independently with the goal of covering 100% of the PTV HR with 95% of the prescription dose; however, when necessary, either the number or fractions or coverage should be reduced using best clinical judgment in order to ensure normal tissue sparing.

## 7.5 Normal Tissue Definitions

Organs at risk (OARs) are defined on treatment planning CTs and co-registered postoperative MRIs. We recommend defining the following structures: retinas/globes, optic nerves, optic chiasm, lenses, lacrimal glands, brain stem, spinal cord, brain, temporal lobes, hippocampi, hypothalamus, pituitary, salivary glands, mandible, oral cavity, larynx, pharyngeal constrictors, and upper esophagus (Table 7.1).

**Table 7.1** Dose-volume histogram planning objectives for sinonasal proton therapy plans

| Structure | DVH point | Limit | Minor deviation | Major deviation |
|---|---|---|---|---|
| PTV | Relative dose at 95% volume | 100% | D95% ≤ 100% | – |
| PTV | Relative dose at 99% volume | 93% | D99% ≤ 93% | – |
| PTV | Relative volume at 110% dose | 20% | V110 ≥ 20% | – |
| Brain stem | Absolute dose at 0.1 cc | 55 Gy | 55 ≤ D0.1 cc < 64 Gy | D0.1 cc ≥ 64 Gy |
| Brain stem | Maximum absolute dose | 60 Gy | 60 ≤ Dmax <67 Gy | Dmax ≥67 Gy |
| Brain stem surface | Absolute dose at 0.1 cc | 55 Gy | 55 ≤ D0.1 cc < 64 Gy | D0.1 cc ≥ 64 Gy |
| Brain stem core | Absolute dose at 0.1 cc | 50 Gy | 50 ≤ D0.1 cc < 60 Gy | D0.1 cc ≥ 60 Gy |
| Spinal cord | Absolute dose at 0.1 cc | 50 Gy | 50 ≤ D0.1 cc < 55 Gy | D0.1 cc ≥ 55 Gy |
| Optic chiasm | Absolute dose at 0.1 cc | 55 Gy | 55 ≤ D0.1 cc < 60 Gy | D0.1 cc ≥ 60 Gy |
| Optic chiasm | Maximum absolute dose | 57 Gy | 57 ≤ Dmax <62 Gy | Dmax ≥62 Gy |
| Optic nerve (left) | Absolute dose at 0.1 cc | 55 Gy | 55 ≤ D0.1 cc < 60 Gy | D0.1 cc ≥ 60 Gy |
| Optic nerve (right) | Absolute dose at 0.1 cc | 55 Gy | 55 ≤ D0.1 cc < 60 Gy | D0.1 cc ≥ 60 Gy |
| Retina (left) | Absolute dose at 0.1 cc | 50 Gy | 50 ≤ D0.1 cc < 60 Gy | D0.1 cc ≥ 60 Gy |
| Retina (right) | Absolute dose at 0.1 cc | 50 Gy | 50 ≤ D0.1 cc < 60 Gy | D0.1 cc ≥ 60 Gy |
| Larynx | Mean absolute dose | 36 Gy | – | Dmean ≥36 Gy |
| Cochlea (left) | Mean absolute dose | 36 Gy | 36 ≤ Dmean <45 Gy | Dmean ≥45 Gy |
| Cochlea (right) | Mean absolute dose | 36 Gy | 36 ≤ Dmean <45 Gy | Dmean ≥45 Gy |
| Parotid (left) | Mean absolute dose | 26 Gy | Dmean ≥26 Gy | – |
| Parotid (right) | Mean absolute dose | 26 Gy | Dmean ≥26 Gy | – |
| Submandibular gland (left) | Mean absolute dose | 40 Gy | Dmean ≥40 Gy | – |

(continued)

**Table 7.1** (continued)

| Structure | DVH point | Limit | Minor deviation | Major deviation |
|---|---|---|---|---|
| Submandibular gland (right) | Mean absolute dose | 40 Gy | Dmean ≥40 Gy | – |
| Cervical esophagus | Mean absolute dose | 50 Gy | Dmean ≥50 Gy | – |
| Oral cavity | Mean absolute dose | 36 Gy | Dmean ≥36 Gy | – |
| Temporal lobe (left) | Relative volume at 20Gy | 10% | V20 ≥ 10% | – |
| Temporal lobe (left) | Absolute volume at 74Gy | 2 cc | V74 ≥ 2 cc | – |
| Temporal lobe (right) | Relative volume at 20Gy | 10% | V20 ≥ 10% | – |
| Temporal lobe (right) | Absolute volume at 74Gy | 2 cc | V74 ≥ 2 cc | – |
| Hippocampus tail (left) | Mean absolute dose | 20 Gy | Dmean ≥20 Gy | – |
| Hippocampus tail (right) | Mean absolute dose | 20 Gy | Dmean ≥20 Gy | – |
| Hippocampus head (left) | Mean absolute dose | 5 Gy | Dmean ≥5 Gy | – |
| Hippocampus head (right) | Mean absolute dose | 5 Gy | Dmean ≥5 Gy | – |
| Pharyngeal constrictors | Mean absolute dose | 50 Gy | 50 ≤ Dmean <60 Gy | Dmean ≥60 Gy |
| Lacrimal gland (left) | Mean absolute dose | 34 Gy | 34 ≤ Dmean <41 Gy | Dmean ≥41 Gy |
| Lacrimal gland (right) | Mean absolute dose | 34 Gy | 34 ≤ Dmean <41 Gy | Dmean ≥41 Gy |
| Hypothalamus | Mean absolute dose | 5 Gy | Dmean ≥5 Gy | – |
| Pituitary | Mean absolute dose | 30 Gy | Dmean ≥30 Gy | – |
| Mandible | Mean absolute dose | 40 Gy | – | Dmean ≥40 Gy |
| Mandible | Relative volume at 70Gy | 10% | – | V70 ≥ 10% |
| Brain | Absolute volume at 74Gy | 2 cc | V74 ≥ 2 cc | – |
| Lens (right) | Maximum absolute dose | 15 Gy | Dmax ≥15 Gy | – |
| Lens (left) | Maximum absolute dose | 15 Gy | Dmax ≥15 Gy | – |

## 7.6 Proton Modality

Both scattered beams and spot-scanning beams can be used, and preferences on modality will depend on the experience of the center, provider, equipment specifications, and most importantly plan quality and robustness. The potential advantages of scanning beams include efficiency of delivery, dose homogeneity, and ability to conform high-dose volumes to concave/convex target volumes. Conversely, it is noteworthy that most of the published outcomes with proton therapy are with the use of passive scattering techniques. The lateral dose gradient will usually be

sharper in a passively scattered beam shaped with a beam aperture especially when compared with pencil-beam systems with larger spot sizes. Also, in scattered proton beams, compensator smearing can be used to yield extremely robust plans despite significant variations in stopping power in areas of bone and air interfaces in the sinus cavities.

For passively scattered beams, aperture margins are customized for each patient to maximize target volume coverage and normal tissue sparing. Typically, 3–5 fields are used per plan (Fig. 7.6). Range modulation is used to ensure that the spread-out Bragg peak (defined as 90% of the mid-spread-out Bragg peak dose) covered the entire radiographic depth of the target volume. An additional distal and proximal margin is added to the CTV if larger than the PTV to account for range uncertainties [10]. Field matching can be used to reduce dose to uninvolved regions and OARs. Through/patch combinations are typically not needed and can be problematic in sinonasal cancer because the target volume and adjacent tissues will inherently involve air cavities which are unsuitable for through/patch junctions. In general, we recommend minimizing the number of field junctions, paying careful attention to uncertainties at junction lines and avoiding/minimizing the number of fields whose distal Bragg peaks end on critical normal tissues such as the spinal cord, brain stem, or visual pathways. The distal dose fall-off of each field is shaped by beam compensators, which can be edited to modify coverage goals or OAR sparing. These compensators also reduce the effects of tissue heterogeneity on the dose distribution. Compensator smoothing/smearing can be used to mitigate the effect of geometric uncertainties on radiographic depth/proton range.

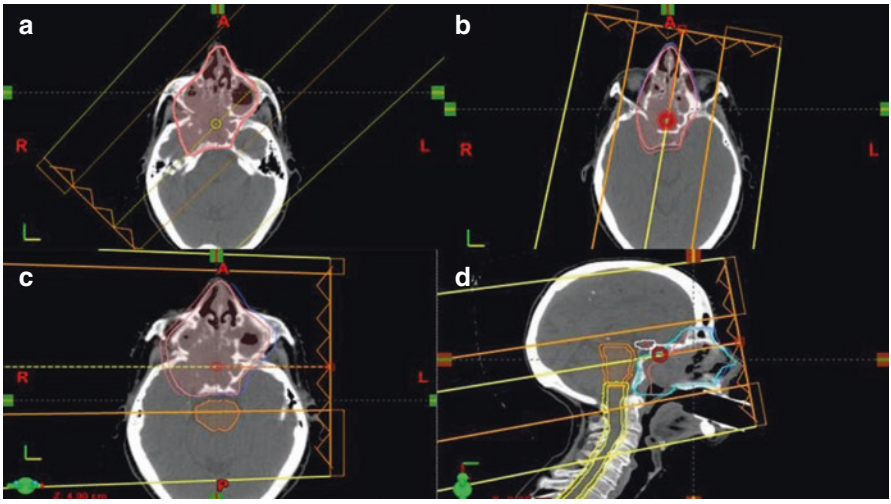


**Fig. 7.6** Example of passively scattered proton therapy plan beam arrangement for a T4b N0 M0 nasal cavity squamous cell carcinoma with intracranial invasion. The beam arrangement includes a right posterior oblique field (**a**), left anterior oblique field (**b**), left lateral field (**c**), and left superior-anterior oblique field (**d**). Fields **a** and **d** cover the entire target volume, while **b** and **c** are matched fields, which can be used to reduce the dose to the eyes

In IMPT plans, typically 3–4 beams are selected, and spot placement and weighting are optimized using inverse planning software. Single-field uniform dose (SFUD) and multi-field optimized (MFO) treatment planning modes can both be used with the former delivering more robust plans, and the latter resulting in improved plan conformality and OAR sparing in plans with PTV convexities/concavities. Plan optimization, similar to IMRT, will be based on objectives for target coverage, OAR sparing, and dose uniformity and their relative weighting within a cost function. Recent advances in treatment planning software now allow for robust plan optimization and plan robustness analysis, which can reduce the impact of geometric/physical uncertainties in the optimization process.

## 7.7 Lymph Node Management

Elective neck irradiation remains a controversial topic in the management of sinonasal cancers. Unlike other more common mucosal cancers of the head and neck, the sinonasal region is relatively devoid of submucosal lymphatic, and lymph node metastases are far less common. Staging evaluation should include imaging of the neck, and clinically and radiographically suspicious lymph nodes, which occur in approximately 10% of patients, should be biopsied to confirm disease [3]. These nodes should be managed with gross total excision and elective dissection of the involved neck and treated with postoperative radiotherapy in a similar manner to other head and neck primary mucosal tumors. The decision to electively irradiate an uninvolved neck is far more controversial and beyond the scope of this chapter. In general, when elective lymphatic irradiation is recommended, we target lymph nodes in the retropharyngeal, retrostyloid regions, and the following cervical lymph node stations: 1b, 2a/b, 3, 4, 5a/b, and the supraclavicular lymph nodes. With well-lateralized tumors that do not invade the nasal septum or cross midline, targeting ipsilateral lymph nodes may be an appropriate volume reduction strategy to minimize potential toxicity.

Different planning strategies for elective lymph node irradiation can be incorporated with proton therapy. Whole neck radiotherapy will typically require IMPT, because the added complexity of treating the neck with passively scattered beam requires prohibitively excessive number of beams and treatment time. We advocate a more simple approach of treating the neck with conventional photon irradiation which can be dosimetrically matched to proton therapy of the primary site and upper neck or with a dosimetric gap to avoid potential hot spots (Fig. 7.7).

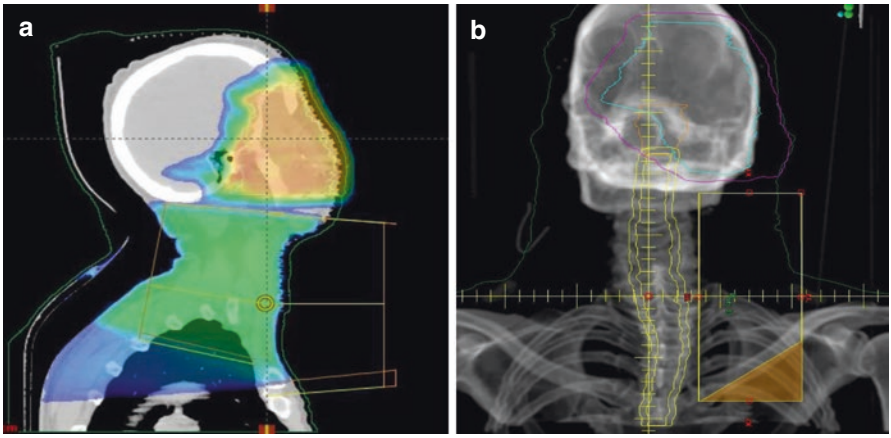


**Fig. 7.7** Photon elective neck irradiation matched to passively scattered proton therapy to the primary site. The 50% isodose level from the proton therapy to the primary site is transferred to the photon treatment planning system in order to create a dosimetric match and avoid hot spot in potential overlap region

## References

1. Turner JH, Reh DD. Incidence and survival in patients with sinonasal cancer: a historical analysis of population-based data. Head Neck. 2012;34(6):877–85.
2. Chu Y, Liu HG, Yu ZK. Patterns and incidence of sinonasal malignancy with orbital invasion. Chin Med J. 2012;125(9):1638–42.
3. Dagan R, Bryant CM, Li Z, et al. Outcomes of sinonasal cancer treated with proton therapy. Int J Rad Biol Phys. 2016;95(1):377–85.
4. Gil Z, Carlson DL, Gupta A, et al. Patterns and incidence of neural invasion in patients with cancers of the paranasal sinuses. Arch Otolaryngol Head Neck Surg. 2009;135(2):173–9.
5. Mendenhall WM, Amdur RJ, Morris CG, Kirwan J, Malyapa RS, Vaysberg M, et al. Carcinoma of the nasal cavity and paranasal sinuses. Laryngoscope. 2009;119(5):899–906.
6. Patel SH, Wang Z, Wong WW, et al.Charged particle therapy versus photon therapy for paranasal sinus and nasal cavity malignant diseases: A systematic review and meta-analysis. Lancet Oncol, 2014:15, pp. 1027–1038.
7. Cannon DM, Geye HM, Hartig GK, Traynor AM, et al. Increased local failure risk with prolonged radiation treatment time in head and neck cancer treated with concurrent chemotherapy. Head Neck. 2014;36(8):1120–5.
8. Mayo C, Martel MK, Marks LB, Flickinger J, Nam J, Kirkpatrick J. Radiation dose-volume effects of optic nerves and chiasm. Int J Radiat Oncol Biol Phys. 2010;76(3 Suppl):S28–35.
9. Monroe AT, Bhandare N, Morris CG, Mendenhall WM. Preventing radiation retinopathy with hyperfractionation. Int J Radiat Oncol Biol Phys. 2005;61(3):856–64.
10. Moyers MF, Miller DW, Bush DA, et al. Methodologies and tools for proton beam design for lung tumors. Int J Radiat Oncol Biol Phys. 2001;49:1429–38.